Neutron powder diffraction study of a system of half-hole-doped bismuth-based calcium manganites at room temperature

2005 J. Phys.: Condens. Matter 17 S3139

(http://iopscience.iop.org/0953-8984/17/40/017)

INSTITUTE OF PHYSICS PUBLISHING JOURNAL OF PHYSICS: CONDENSED MATTER

J. Phys.: Condens. Matter **17** (2005) S3139–S3147 doi:10.1088/0953-8984/17/40/017

Neutron powder diffraction study of a system of half-hole-doped bismuth-based calcium manganites at room temperature

K A Krezhov[1], D Kovacheva[2], E Sváb[3] and F Bourée[4]

[1] Institute for Nuclear Research and Nuclear Energy, 72 Tzarigradsko Chaussée, BG-1784 Sofia, Bulgaria
[2] Institute of General and Inorganic Chemistry, Academician G.Bontchev, Boulevard 11, BG-1113, Sofia, Bulgaria
[3] Research Institute for Solid State Physics and Optics, 1525 Budapest, POB 49, Hungary
[4] Laboratoire Leon Brillouin (CEA-CNRS), CEA/Saclay, 91191 Gif-sur-Yvette, France

Received 8 July 2005
Published 23 September 2005
Online at stacks.iop.org/JPhysCM/17/S3139

Abstract

The structural effects of partial replacement of diamagnetic Bi^{3+} for potential charge ordering and magnetic ordering phenomena in $Bi_{0.25}R_{0.25}Ca_{0.5}MnO_3$ (R = La, Nd, Ho) have been studied. The analysis of the room-temperature data suggests that in bismuth-based calcium perovskites the lone pair character of $6s^2$ Bi^{3+} orbitals is constrained rather than dominant. At 10 K the ground magnetic state of all compounds was specified as CE-type antiferromagnetic.

(Some figures in this article are in colour only in the electronic version)

1. Introduction

Manganese oxide materials are attracting significant interest, stimulated by the rediscovery of the colossal magnetoresistance (CMR) effect in the perovskite systems of the $R_{1-x}A_xMnO_3$ type, where R stands for La^{3+}, Pr^{3+} and heavier rare-earths, A = Ca^{2+}, Sr^{2+}, Ba^{2+}, Pb^{2+}, and manganese is in its two valence forms Mn^{3+} and Mn^{4+}. It was established that the large change of electrical resistivity under the action of applied magnetic field is preserved in thin films, thus providing a broad area of possible technological applications [1]. Intensive investigation of the structural impact on magneto-transport properties has revealed that the specific crystal structure and the oxygen octahedral configuration in particular, the type of long-range ordering of magnetic moments, local structural and magnetic disorder, charge ordering on manganese cations, and the strong electron–phonon coupling are the main factors that interplay [2, 3].

One of the most interesting current topics in manganese oxides apart from the CMR effect is the problem of charge-ordered (CO) configurations as well as possible intrinsic phase segregation phenomena [4]. Understanding the charge–orbital ordering (CO/OO) and the complex relationships between their structural phenomena and physical properties

is a real challenge. For phases displaying coherent orbital ordering (OO) the diffraction techniques provide a means to detect the full extent of the concomitant lattice distortions. For half-hole doping ($x = 1/2$) it is expected that the CE-type antiferromagnetic (AFM) phase (e.g. [2–4]) is attained at T_N on cooling a CO/OO state already set in at a certain temperature $T_{CO} \geqslant T_N$. It is worth noting that there are two distinct structural models giving alternative superstructures of the CO-phase in half-doped manganites. The ordered Zener polaron (ZPO) model (e.g. [5]) describes an electronic state in which the manganese ions have an intermediate valence of 3.5 throughout the structure. The conventional OO/CO ionic model (e.g. [3]) assumes $Mn^{3.5+\delta}/Mn^{3.5-\delta}$ charge disproportionation. The extremes of the latter are separated and spatially ordered Mn^{3+} and Mn^{4+} ionic species. A phenomenological approach to the phase transition (PT) in the frame of Landau theory allows viewing the low-symmetry phase as the outcome of a PT for both models [6]. Therefore, a key role in the understanding of the relationships between local and average structure is played by the so-called charge-ordered compounds, like $La_{0.5}Ca_{0.5}MnO_3$, $Pr_{0.5}Ca_{0.5}MnO_3$, $Pr_{2/3}Ca_{1/3}MnO_3$, $Nd_{0.5}Ca_{0.5}MnO_3$ and just a few others. For $La_{0.5}Ca_{0.5}MnO_3$ it has been shown that charge and magnetic ordering are associated with orbital ordering, whereby the Jahn–Teller (JT)-distorted MnO_6 octahedra form a long-range-ordered quasicommensurate superstructure [7]. On the other hand, $Pr_{0.5}Sr_{0.5}MnO_3$ displays an A-type AFM order at low temperatures with no sign of charge ordering but exhibiting orbital order, while $Pr_{0.5}Ca_{0.5}MnO_3$ ($T_{CO} = 230$ K, $T_N = 180$ K) is considered as a paradigmatic example of the $x = 1/2$ CO/OO materials. The OO, CO and the CE-type magnetic structures have been shown from additional studies on $La_{0.5}Ca_{0.5}MnO_3$ [8] and $Nd_{0.5}Ca_{0.5}MnO_3$ [9] to be sensitive to oxygen stoichiometry and annealing conditions.

It is worth noting that among the many perovskite oxides the bismuth-based manganites have not been extensively investigated, although the presence of OO/CO effects was suggested long ago [10]. Recent structural characterizations by electron [11] and neutron [12] diffraction studies showed OO/CO at room temperature for $Bi_{0.5}Ca_{0.5}MnO_3$ ($T_{CO} = 335$ K) and $Bi_{0.5}Sr_{0.5}MnO_3$ and proved in the latter the anomalously high $T_{CO} = 475$ K. In reasoning the findings, attention was drawn to the possible role of the Bi^{3+} lone electron pair in the phase transition. In both compounds, the modulation vector is parallel to the reciprocal lattice parameter a^* and the amplitude close to 0.5, i.e. involves a doubling of a cell parameter (in the *Pnma* space group setting). The ordering phenomena were described in the OO/CO model [13] and later reexamined in terms of the ZPO model (e.g. references cited in [14]). In fact, in [13] from neutron powder diffraction data on $Bi_{0.5}Sr_{0.5}MnO_3$ the AFM CE-type magnetic structure was detected below $T_N = 155$ K in the presence of a minor AFM phase with A-type ordering. The finding is in support of the phase separation conception. However, in [14] a one-phase description of the neutron and magneto-transport single-crystal data was found sufficient by arguing that in [13] the A-type order most probably was set in a minor part of the sample slightly richer in Mn^{4+}.

We undertook this study on $Bi_{0.25}R_{0.25}Ca_{0.5}MnO_3$ (R = La, Nd, Ho) with the aim of specifying the structural effects of partial replacement of diamagnetic Bi^{3+} for potential CO and magnetic ordering phenomena. Some results of this work related to $Bi_{0.25}Ho_{0.25}Ca_{0.5}MnO_3$ have been reported in [15, 16]. The main objective is to facilitate the understanding of the origin of the MR, OO and CO effects in half-hole-doped compounds as well as the relation to macroscopic phase separation phenomena.

2. Experimental section

Polycrystalline $Bi_{0.25}R_{0.25}Ca_{0.5}MnO_3$ material was prepared by the standard solid-state reaction in air from mixtures of high-purity grade materials Bi_2O_3, $CaCO_3$, $MnCO_3$ and

R_2O_3 (R = La, Nd, Ho; desiccated at 800 °C for 3 h before weighing), taken in appropriate weight ratios near to stoichiometric proportion with accounting for the volatility of bismuth. The mixtures, thoroughly ground under ethanol in an agate mortar, were preheated in air for 6 h at 800 °C twice, with intermediate grinding, to ensure carbonate decomposition. The products were reground, pressed into pellets under 430 MPa, loaded in platinum crucibles, and heated in air at 900 °C for 15 h, 1000 °C for 24 h, and 1250 °C for 36 h with repeated intermediate regrinding and pressing. The cooling rate was near 200 °C h^{-1}. X-ray powder diffraction analyses were performed at room temperature for phase control of precursors and final products until the formation of a nominally single-phase material was completed. The phase purity was also confirmed by the neutron experiments. Iodometric titration gave an oxygen content of 3 within 1.5% limit of accuracy.

Neutron powder diffraction (NPD) measurements were carried out using the medium-resolution diffractometer PSD at the Budapest Neutron Centre and the high-resolution diffractometer 3T2 at the Laboratoire Leon Brillouin (CEA/Saclay). The PSD data (λ = 1.0577 Å) were collected with the sample in a thin-walled vanadium can at room temperature (RT) in the range $4.5° < 2\theta < 113.6°$ with an angular step of 0.1°. The 3T2 instrument patterns (λ = 1.2251 Å) were recorded using a cryofurnace at 292 K and at 10 K in the range $6° < 2\theta < 125.6°$ with a step of 0.05°. The data were analysed by the Rietveld method using the FullProf software suite [17] with the built-in neutron scattering amplitudes and magnetic form factors. A linear interpolation of fixed points was used to model the background. An absorption correction was introduced on the basis of transmission measurements using the PSD. Magnetic susceptibility data were collected using a Faraday translational magnetic balance. Magnetization measurements were performed on a vibrating sample magnetometer down to 77 K. The zero-field resistivity was measured by a standard four-probe method on sintered bars with dimensions $1.8 \times 2 \times 8$ mm^3. All the experiments were performed on heating after the sample was zero-field cooled down to the low temperature.

3. Results and discussion

The measurements in the range 77 K < T < 1000 K evidenced the Curie–Weiss behaviour of magnetic susceptibility at sufficiently high temperatures only, $T > 550$ K. The asymptotic paramagnetic temperatures θ_p were all positive, indicating the presence of ferromagnetic correlations. However, a clear ferromagnetic response appeared only for $Bi_{0.25}La_{0.25}Ca_{0.5}MnO_3$ (BLCMO) at $T_C = 281 \pm 5$ K. For $Bi_{0.25}Nd_{0.25}Ca_{0.5}MnO_3$ (BNCMO) and $Bi_{0.25}Ho_{0.25}Ca_{0.5}MnO_3$ (BHCMO) in the field-induced magnetization there was a kink in vicinity of 100 K, which might be a sign for the onset of long-range AFM ordering. For BCMO, which is known to adopt the CE AFM ordering at low T, a similar kink appeared at 125 ± 5 K.

$La_{0.50}Ca_{0.50}MnO_3$ (LCMO) has long been considered as an example for the strong competition between double-exchange-driven FM and superexchange-driven AFM interactions. The FM and AFM states appear successively upon cooling. At high temperatures, LCMO is a paramagnetic insulator, and upon cooling it first becomes FM and metallic (T_c = 225 K) and then AFM–CO insulator ($T_N \approx 195$ K), $T_N \approx T_{CO} = 210$ K. The CO to charge disorder transition is first order, and displays hysteresis as extracted from ZF-μSR and dc magnetization measurements. On the other hand, $Nd_{0.5}Ca_{0.5}MnO_3$ is an insulator over the entire temperature range, from 300 K down to 4.2 K, with CE AFM magnetic moments along the a axis. In contrast with LCMO. the samples BCMO, BLCMO, BNCMO and BHCMO did not exhibit the insulator–metal transition and they remained semiconductors down to 77 K. Moreover, the application of a magnetic field of 1 T did not appreciably change the resistivity

of the samples studied. At RT the value of resistivity of BCMO was about four orders of magnitude lower than that of LCMO and the change in the resistivity measured at T_{CO} and T_N was much less abrupt when compared to most of the hole-doped rare-earth-based manganites exhibiting CO/OO phenomena.

At RT all of the Bi–Ca compounds investigated adopt structures which can be satisfactorily described in orthorhombic *Pnma* space group. At 10 K the CE AFM ordering was established, but details of concomitant structural changes are beyond the scope of the present study and will be published elsewhere.

It is worth noting that the (1/2 2 2) superlattice Bragg reflection observed to evolve with temperature for $La_{0.5}Ca_{0.5}MnO_3$, $Pr_{0.5}Ca_{0.5}MnO_3$, and $Nd_{0.5}Ca_{0.5}MnO_3$ and expected for BCMO at RT to appear at $2\theta = 28.15°$ as evidence for the existence of the particular OO structural transition (structural modulation with $k = (1/2, 0, 0)$ wavevector) with entailed doubling of the unit cell in the *a* direction was hardly seen. In fact, the NPD pattern of BCMO at RT did not present clear superlattice peaks but refinements in monoclinic space group $P12/m1$ providing two distinct sites for manganese, even without doubling the *a* parameter, produced slightly better results in terms of conventional agreement factors.

Figure 1 exemplifies for the BNCMO case the observed neutron pattern and the refined fit to the diffraction data. Table 1 summarizes our results determined from the Rietveld refinements of the NPD patterns at RT considering the averaged unit cell and similar structural results available on some Ln–Ca (Ln = La, Nd) manganites [18].

The first thing to note is that unlike the La-substituted analogues, the Bi-based compounds feature low lattice degeneracy; the three orthorhombic lattice parameters are significantly different, which is a considerable advantage for high-resolution powder diffraction studies. In this sense, the compound BNCMO is an appealing test system, because the A-site cationic mismatch defined through ionic size variance $\sigma^2 = \langle r_A^2 \rangle - \langle r_A \rangle^2$ [19] should be minimal in the case of the constrained lone-pair character of Bi. As discussed below, if the Bi lone-pair character were constrained the two cations Bi^{3+} and Nd^{3+} would have almost identical ionic radii ($r_{Nd} \approx 1.163$ Å).

The data show that the unit cell of all Bi-based compounds is already anisotropically distorted, suggesting that the orbital order most probably exists in close proximity to RT. The unit cell parameters $b/\sqrt{2} \leqslant c \leqslant a$ in all cases characterize O-type distorted perovskite structures. In addition, as illustrated by figures 2(a)–(c), there is a strong anisotropic distortion of the MnO_6 octahedra which is usually associated to the particular orbital order present at this doping level ($x = 1/2$).

We recall that Bi^{3+} and La^{3+} have very similar radii in many oxides [20]. However, Bi^{3+}, in contrast to La^{3+} and other rare-earth cations, has a highly polarizable $6s^2$ electron pair and its effective volume varies depending whether the lone-pair character is dominant or not. In ninefold coordination, which is used usually for comparison in manganites, for $6s^2$ character dominant Bi^{3+} has nearly the same size as La^{3+} ($\langle r_{Bi} \rangle^{IX} \approx 1.24$ Å), for $6s^2$ character constrained, $\langle r_{Bi} \rangle \approx 1.16$ Å. It is worth noting that theoretical studies indicate that when the lone pair is weakly screened 6s-Bi orbitals can hybridize with 2p-O orbitals, thus reducing the mobility of Mn e_g electrons through Mn–O–Mn bridges.

Figures 2(a)–(c) provide strong evidence that to a great extent the stability of the OO/CO state in Bi-based manganites could be attributed to the larger bending of the exchange Mn–O–Mn angle when compared to La-based compounds. The replacement of La by Bi in the $x = 1/2$ (Ca) compounds leads to a significant decrease of the mean bond angle ⟨Mn–O–Mn⟩; for BCMO this decrease is of about 5° in comparison with LCMO. Undoubtedly, the reason for those differences should be connected with the role that Bi plays in these compounds. It is worth recalling that the Bi ion is more electronegative than rare-earths (Pauling electronegativity for

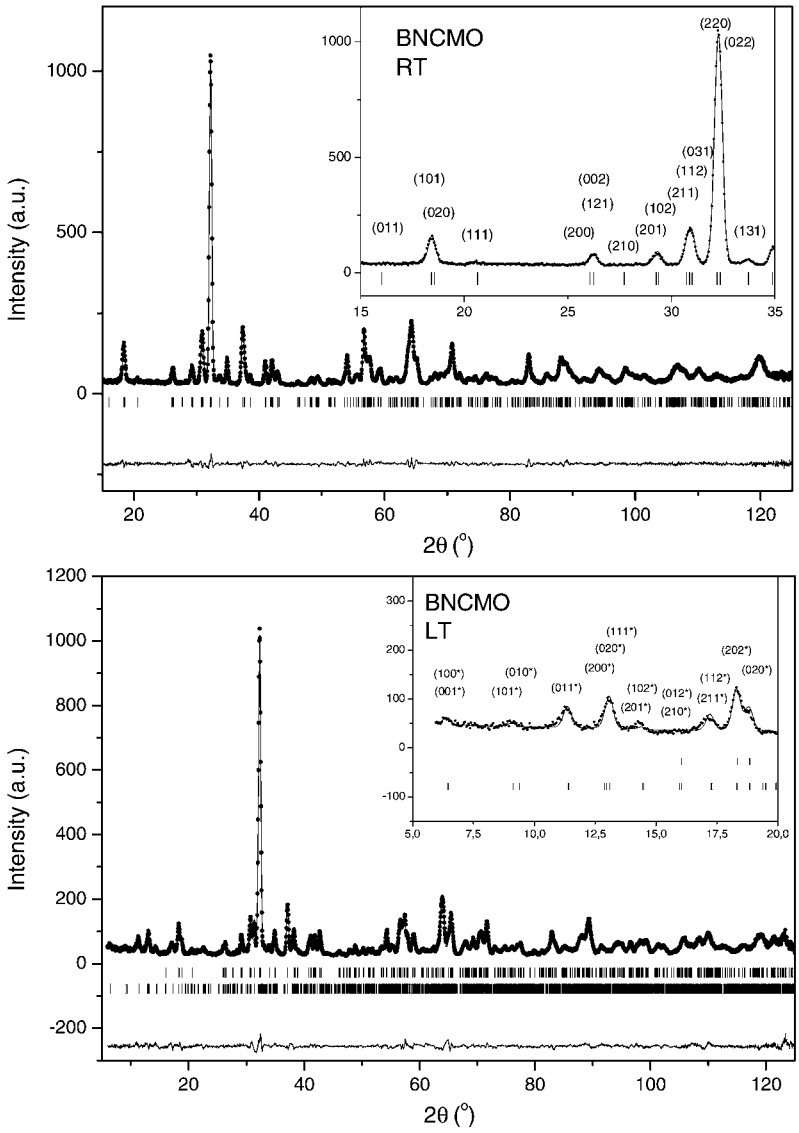

Figure 1. Experimental, calculated and difference (bottom) neutron diffraction patterns of $Bi_{0.25}Nd_{0.25}Ca_{0.5}MnO$ registered on the 3T2 high-resolution diffractometer at room temperature (RT) and 10 K (LT). The tick marks below the profile indicate the position of allowed Bragg reflections. The inset shows the low-angle region of the corresponding pattern in detail. The magnetic reflections (marked by asterisks) at 10 K have been indexed using the lattice parameters ($2a$, b, $2c$) of the magnetic unit cell.

Bi $\approx$ 2.02 and for La and Pr $\approx$ 1.10–1.13) and than manganese (Pauling electronegativity for Mn $\approx$ 1.55), and this enhances the Bi–O hybridization and reduces the amount of Mn–O hybridization.

The inspection of the Mn–O bond distances gives grounds to conclude that the octahedra are rather different in the two families of perovskites. The mean Mn–O distance in Bi–Ca compounds is larger than that in Ln–Ca compounds. The Mn–O angles indicate that the

Table 1. Selected structural parameters as refined in orthorhombic space group *Pnma* for $Ln_{0.5}Ca_{0.5}MnO_3$ (Ln = La, Nd, Bi), $La_{0.25}Nd_{0.25}Ca_{0.5}MnO_3$, and $Bi_{0.25}Ln_{0.25}Ca_{0.5}MnO_3$ (Ln = La, Nd, Ho). Estimated standard deviations are in parentheses. The parameters characterizing the distortion of MnO_6 octahedron Δ, ε_d are defined as $\Delta = (1/N)\sum_n[(d_n - \langle d\rangle)/\langle d\rangle]^2$ and $\varepsilon_d = |\langle d_{equat}\rangle/d_{apical} - 1|$. (Notes. (1) The data for $La_{0.5}Ca_{0.5}$, $La_{0.25}Nd_{0.25}$, and $Nd_{0.5}Ca_{0.5}$ are taken from Woodward [18]. (2) For $La_{0.5}Ca_{0.5}$, Radaelli *et al* [7] give $a = 5.4248(1)$, $b = 7.6470(2)$, $c = 5.455(1)$, $V_0 = 225.485(9)$; $d_{Mn-O1} = 1.9406(3)$; $d_{Mn-O2} = 1.944(2)$, 1.946(2); $\langle d_{equat}\rangle = 1.945(2)$; $\langle d_{Mn-O}\rangle = 1.9428(7)$.)

Site/comp	$La_{0.5}Ca_{0.5}$	$Bi_{0.5}Ca_{0.5}$	$La_{0.25}Nd_{0.25}$	$Bi_{0.5}La_{0.5}$	$Nd_{0.5}Ca_{0.5}$	$Bi_{0.25}Nd_{0.25}$	$Bi_{0.25}Ho_{0.25}$
			Unit cell dimensions				
a (Å)	5.418 22(4)	5.4740(8)	5.4077(2)	5.432 70(26)	5.392 00(6)	5.4299(2)	5.4531(4)
b (Å)	7.638 90(4)	7.5348(8)	7.6246(1)	7.616 24(31)	7.589 72(8)	7.5944(3)	7.5168(5)
c (Å)	5.426 91(4)	5.4198(7)	5.4047(2)	5.416 80(26)	5.337 605(6)	5.3910(2)	5.3502(9)
V_0 (Å^3)	224.616(3)	223.54(8)	222.840(5)	224.129(18)	220.008(5)	222.286(15)	219.30(3)
			Mean size of A-site cation				
$\langle r_A\rangle$ (Å)	1.198	1.17[c]/1.21[d]	1.185	1.184[c]/1.204[d]	1.172	1.171[c]/1.101[d]	1.148[c]/1.168[d]
			Bond distance (Å)				
d_{Mn-O1} (apical) × 2	1.946(1)	1.929(1)	1.940(1)	1.932(1)	1.936(2)	1.936(1)	1.930 (1)
d_{Mn-O2} (equat) × 2	1.946(1)	1.959(4)	1.961(8)	1.949(3)	1.957(6)	1.954(2)	1.957(2)
	1.937(5)	1.975(4)	1.928(8)	1.962(3)	1.925(6)	1.957(2)	1.965(2)
$\langle d_{Mn-O}\rangle$	1.943(4)	1.954(2)	1.943(6)	1.948(3)	1.939(5)	1.949(2)	1.951(2)
Δ ($\times 10^6$)	4.8	95.2	49.3	39.5	46.9	22.6	58.9
ε_d ($\times 10^4$)	23	197	23	122	26	101	161
			Bond angle (deg)				
Mn–O1–Mn × 2	158.0(3)	155.19(6)	158.5(4)	160.45(3)	157.2(4)	157.40(3)	153.61(4)
Mn–O2–Mn × 4	161.8(1)	156.31(2)	158.8(3)	157.55(10)	157.5(2)	155.93(8)	153.80(4)
⟨Mn–O–Mn⟩	160.5(2)	155.75(4)	158.7(3)	158.52(8)	157.4(3)	156.42(7)	153.73(4)
O1–Mn–O2 × 2	89.0(2)	89.03(23)	89.6(3)	89.19(17)	89.7(2)	89.79(11)	88.79(15)
	89.3(1)	89.56(23)	89.3(3)	88.41(17)	89.7(3)	89.15(13)	89.31(18)
O2–Mn–O2 × 2	89.03(3)	89.22(27)	88.86(8)	89.07(18)	88.90(6)	89.22(12)	89.62(17)

octahedra in Bi compounds exhibit larger Mn–O bond distance mainly due to the expansion of the octahedra in the basal plane.

From the relationship between mean bonding angle ⟨Mn–O–Mn⟩ and mean bond distance $\langle d_{Mn-O}\rangle$ one might infer that the effective ionic radius of Bi^{3+} is less than $\langle r^{+3}_{Bi}\rangle^{ix} = 1.24$ Å which would be expected if the $6s^2$ lone-pair character were dominant. For the dominant lone-pair character, the $6s^2$ electron pair is weakly screened and presumably the electron density of the lone pair is highly along some Bi–O bonds, producing a larger effective Bi^{3+} ionic size. In contrast, for lone-pair character constrained the $6s^2$ orbitals tend to point outwards from the Bi–O bonds, producing a smaller effective Bi^{3+} ionic radius. In addition, figures 3(a) and (b) which present the results for the MnO_6 distortion parameter Δ in the light of constrained ($\langle r^{+3}_{Bi}\rangle^{ix} = 1.16$ Å) and dominant ($\langle r^{+3}_{Bi}\rangle^{ix} = 1.16$ Å) character of the $6s^2$ electron pair of bismuth, is also in support of the similarity between the effective ionic radii of Bi and Nd in the Ca manganites studied.

4. Conclusions

In conclusion, our NPD study on the ternary system $(BiLn)_{0.5}Ca_{0.5}MnO_3$ reveals that, by keeping constant electron concentration, the A-cation size variation in the half-hole-

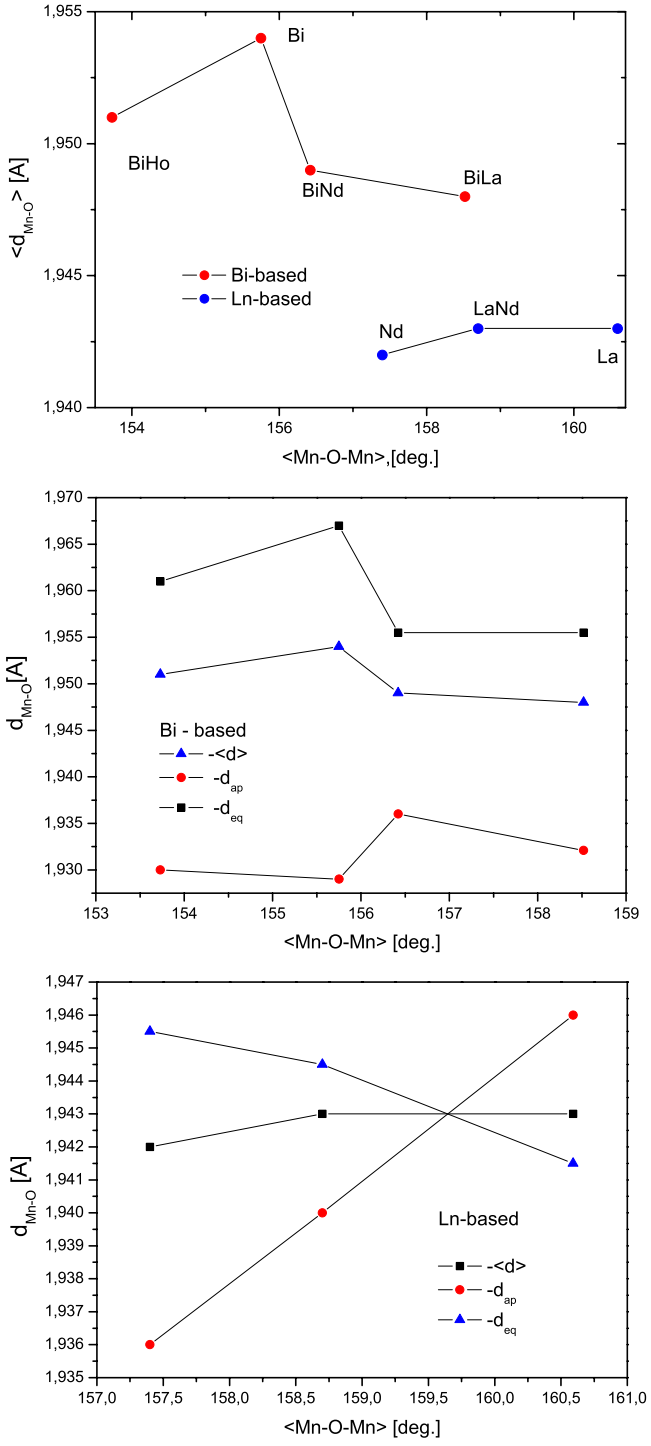

Figure 2. Mn–O distances (see text) and mean angles ⟨Mn–O–Mn⟩ in the families of Bi–Ln–Ca compounds investigated.

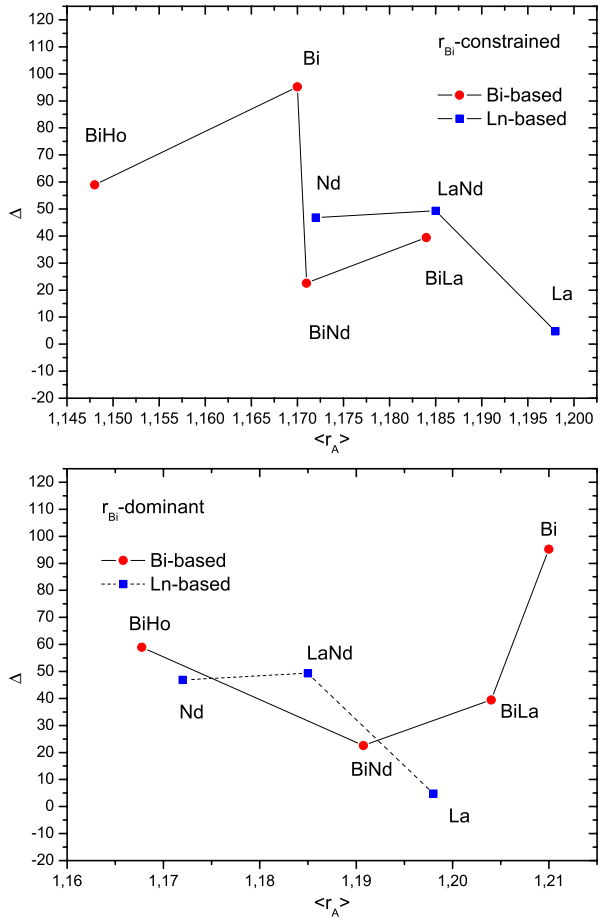

Figure 3. Distortion of MnO_6 octahedra and mean angles ⟨Mn–O–Mn⟩ in the families of Bi–Ln–Ca compounds investigated.

doped $Bi_{0.5}Ca_{0.5}$ manganite leads to substantial structural changes, and the related ground antiferromagnetic state was specified as CE-type antiferromagnetic. The analysis suggests that in bismuth calcium perovskites the lone-pair character of $6s^2$ Bi^{3+} orbitals is constrained rather than dominant.

Acknowledgments

This study was supported in part by the Bulgarian National Fund for Science (contract F-1202/02), the Hungarian OTKA-T42495, and the European Commission through R113-CT-2003-505925.

References

[1] Haghiri-Gosnet A M and Renard J-P 2003 *J. Phys. D: Appl. Phys.* **36** R127–50
[2] Tokura Y and Tomioka Y 1999 *J. Magn. Magn. Mater.* **200** 1
[3] Salamon M B 2001 *Rev. Mod. Phys.* **73** 583

[4] Dagotto E 2002 *Nanoscale Phase Separation and Colossal Magnetoresistance* (Berlin: Springer)
[5] Daoud-Aladin A, Rodríguez-Carvajal J, Pinsard-Gaudart L, Fernandez-Diaz M and Revcoleschi A 2002 *Appl. Phys.* A **71** S.1758
Daoud-Aladin A, Rodríguez-Carvajal J, Pinsard-Gaudart L, Fernandez-Diaz M and Revcoleschi A 2003 *Phys. Rev. Lett.* **89** 097205
[6] Shakhmatov V S, Plakida N M and Tonchev N S 2003 *JETP Lett.* **77** 15
[7] Radaelli P, Cox D, Marezio M and Cheong S W 1997 *Phys. Rev.* B **55** 3015
[8] Barnabe A, Hervieu M, Martin C, Maignan A and Raveau B 1998 *J. Appl. Phys.* **84** 5506
[9] Frontera C, Garcia-Munoz J I, LLobet A, Ritter C, Alonso J A and Rodriguez-Carvajal J 2000 *Phys. Rev.* B **62** 3002
[10] Bokov V, Grigoryan N and Bryzhnina H 1967 *Phys. Status Solidi* **20** 745
[11] Hervieu M, Maignan A, Martin C, Nguyen N and Raveau B 2001 *Chem. Mater.* **21** 1356
[12] Frontera C, García-Muños J, Aranda M, Richter C, Llobet A, Respaud M and Vanacken J 2001 *Phys. Rev.* B **64** 054401
[13] García-Muñoz J L, Frontera C, Aranda M, Llobet A and Richter C 2001 *Phys. Rev.* B **63** 064415
[14] Hejtmánek J, Knížek K, Jirák Z, Damay F, Hervieu M, Martin C, Nevřiva M and Beran P 2003 *J. Appl. Phys.* **93** 7370
[15] Krezhov K, Kovacheva D, Sváb E, Bourée F and Stamenov P 2004 *Physica* B **350/1-3S** E13–7
[16] Krezhov K 2003 *(A-24)* pp 2203–08 http://www.phy.bg.ac.yu/~bpu5/proceedings/appendix
[17] Rodriguez-Carvajal J 1993 *Physica* B **192** 55
[18] Woodward P M, Vogt T, Cox D, Arulraj A, Rao C N R, Karn P and Cheetham A K 1998 *Chem. Mater.* **10** 3652–65
[19] Damay F, Martin C, Maignan A and Raveau B 1997 *J. Appl. Phys.* **82** 6181–5
[20] Shannon R D 1976 *Acta Crystallogr.* A **32** 751